



Roman Skibiński · Jacek Golak · Volodymyr Soloviov ·  
Kacper Topolnicki · Yuriy Volkotrub · Henryk Witała

# Modern Chiral Forces Applied to the Neutron-Deuteron Breakup Reaction

Received: 18 June 2021 / Accepted: 8 July 2021 / Published online: 23 July 2021  
© The Author(s) 2021

**Abstract** We report on applications of the recent chiral potentials from the Bochum-Bonn group to the description of the neutron induced deuteron breakup observables. Specifically, we discuss the convergence of predictions with respect to the chiral order and the dependence of our results on the value of the regularization parameter. To that end we use the chiral forces with semi-local coordinate or momentum space regularization up to the  $N^4LO^+$  order of chiral expansion. We find a satisfactory picture revealing high quality of the chiral forces used.

## 1 Introduction

After a long period of research focused on the phenomenological or meson-exchange based models, investigations of nuclear forces got a new impetus with the development of the chiral perturbation theory. Starting from the seminal paper by S. Weinberg [1] many groups took up the challenge to construct nuclear chiral potentials, see for example the review papers [2, 3]. The contribution of the Bochum-Bonn group has been very important. Already in 1998 E. Epelbaum and collaborators presented a chiral nucleon-nucleon (NN) interaction [4–6]. In the next step they constructed a chiral three-nucleon force (3NF), which allowed them to apply successfully chiral interactions to study the nucleon-deuteron (Nd) elastic scattering and the deuteron breakup [7]. These nuclear forces were later applied to other systems and processes, including nuclear structure investigations [7] or reactions with electroweak probes [8, 9]. In those early works the non-local regularization of the NN and 3N potentials was used. However, after applying higher-order chiral components it became clear, that a more sophisticated way of regularization is required [10–12]. Meeting this requirement E. Epelbaum and collaborators proposed firstly a new interaction with a semi-local regularization applied in coordinate space (SCS) [13–15] and later the so-called SMS force [16] for which the semi-local regularization was applied directly in momentum space. Very recently the 3NF consistent with the SMS NN force have been also derived at the third order of chiral expansion ( $N^2LO$ ) [24]. Of course, the regularization is not the only difference between mentioned above potentials. Few other improvements and developments introduced in the SMS force [16] are: fixing the pion-nucleon low energy constants using the Roy-Steiner analysis [17], removing redundant structures at the higher orders of the chiral expansion, using the Granada self-consistent data base [18] to fix free parameters of the potential and availability of covariance matrix of potential parameters. The latter has been recently used for estimation some theoretical uncertainties of Nd observables [19] as well as to study correlations among 3N observables [20]. The SMS NN force at the fifth order of the chiral expansion ( $N^4LO$ ) has been supplemented by additional  $N^5LO$  F-wave contact terms which led to the  $N^4LO^+$  interaction. Resulting description of the NN data is impressive, yielding the  $\chi^2/\text{data}$  values  $\approx 1.0$ , depending

on the isospin, regulator value and energy range [16]. For example, the  $N^4LO^+$  neutron-proton force describes NN data up to 300 MeV with  $\chi^2/data=1.06$ .

The 3N interaction has been also evolving and the recent  $N^2LO$  version, consistent with the SMS NN force is given in [21]. It has two free parameters, whose values have been fixed from the  $^3H$  binding energy and the Nd elastic scattering differential cross section at  $E=70$  MeV. Currently the 3NF consistent with the NN SMS interaction is available for practical computations at  $N^2LO$  only.

In the following we focus on the most recent versions of the chiral potentials from the Bochum-Bonn group. In Chapter 3 we give a few examples of predictions on observables in the deuteron breakup at energies of incoming neutron up to 135 MeV. These predictions have been obtained within the Faddeev formalism [22], briefly described in Chapter 2. For results on Nd elastic scattering we refer to [7, 19, 21].

## 2 Formalism

Our computations are conducted in momentum space, neglecting the proton-proton Coulomb force for the proton-deuteron system. The complete Faddeev equation [22, 23] when both NN and 3N forces act reads

$$T|\psi\rangle = tP|\psi\rangle + tPG_0T|\psi\rangle + (1+tG_0)V_4^{(1)}(1+P)|\psi\rangle + (1+tG_0)V_4^{(1)}(1+P)T|\psi\rangle \quad (1)$$

and its solution for the auxiliary state  $T|\psi\rangle$  allows us to find observables for the Nd breakup reaction via the transition operator  $U_0 = (1+P)T$ .

The NN interactions  $V$  together with the two-nucleon free propagator  $\tilde{G}_0$  defines the  $t$ -operator via the Lippmann-Schwinger equation

$$t = V + V\tilde{G}_0t. \quad (2)$$

In Eq. (1) the  $V_4^{(1)}$  is a part of the 3NF which is symmetrical under the exchange of nucleons 2 and 3. Further, the initial state  $|\psi\rangle$  is composed of the deuteron and a momentum eigenstate of the projectile nucleon,  $P$  is a permutation operator which is used to account for indistinguishability of the nucleons and  $G_0$  is the free 3N propagator.

We solve Eq. (1) with the partial wave scheme. We work in the  $|p, q, \alpha\rangle$  basis states with  $p = |\mathbf{p}|$  and  $q = |\mathbf{q}|$  being the magnitudes of the Jacobi momenta  $\mathbf{p}$  and  $\mathbf{q}$ . The set of discrete quantum numbers  $\alpha$  comprises the ones used in the  $jI$ -coupling scheme

$$\alpha = \left( (l, s)j; (\lambda, \frac{1}{2})I; (j, I)JM_J; (t, \frac{1}{2})TM_T \right), \quad (3)$$

with  $l, s, j, \lambda, I, J, M_J, t, T, M_T$  denoting the relative orbital angular momentum in the 2-3 subsystem, total spin of the 2-3 subsystem, total angular momentum of the 2-3 subsystem, the orbital and total angular momenta of particle 1 with respect to the centre of mass of the 2-3 subsystem, total angular momentum of 3N system, its projection, isospin of the 2-3 subsystem, total isospin of 3N system and its projection, respectively. After expressing operators of Eq. (1) in the partial wave basis  $|p, q, \alpha\rangle$ , we solve Eq. (1) generating its Neumann series and perform Pade summation. We take into account all partial waves with  $j \leq 5$  and  $J \leq \frac{25}{2}$ . These values are sufficient to obtain fully converged solutions at the presented here energies.

## 3 Results

We start with a comparison of various predictions for the neutron-deuteron breakup process at the laboratory kinetic energy of  $E=65$  MeV. At this relatively low energy we may restrict ourselves to complete  $N^2LO$  calculations. We use various chiral forces: the SCS NN+3NF, the SMS NN+3NF as well as the SMS NN+3NF (SMS-org) for which the 3NF is taken in its original form of Ref. [24]. We chose the cutoff parameter  $\Lambda = 450$  MeV ( $R = 0.9$  fm) for the SMS (SCS) force. In Fig. 1 we show the differential cross section  $\frac{d^5\sigma}{d\Omega_1 d\Omega_2 dS}$  for two kinematical configurations defined by directions of laboratory momenta of two outgoing neutrons  $(\theta_1, \phi_1)$  and  $(\theta_2, \phi_2)$ .  $S$  shows the position on the S-curve collecting all kinematically allowed events in the  $E_1 - E_2$  plane, see [22] for definition and used convention. We observe that both curves, representing the SCS and the SMS-org based predictions are close to each other and to the centre of the dark green band which corresponds to predictions of the SMS potential. In addition to this agreement, it can be seen that all curves

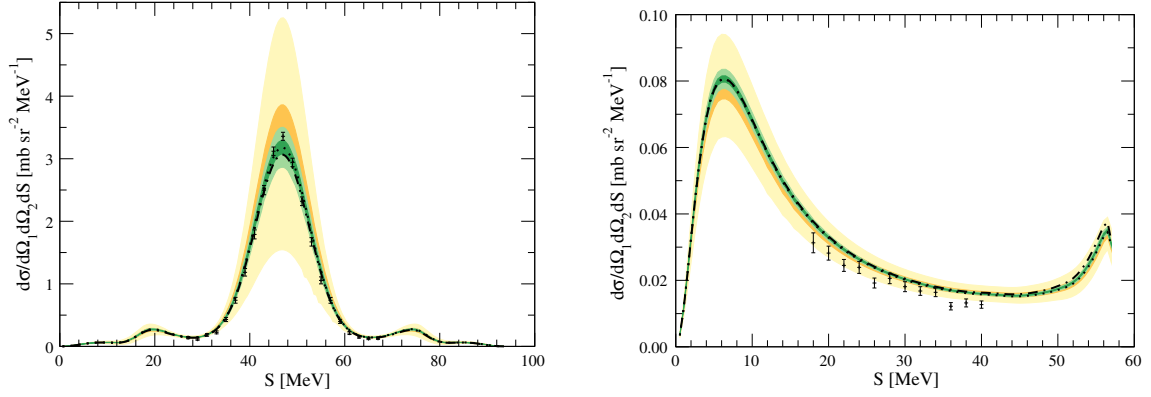


**Fig. 1** The differential cross section  $\frac{d^5\sigma}{d\Omega_1 d\Omega_2 dS}$  for the  $d(n, n_1 n_2)p$  reaction for two kinematical configurations given by directions of momenta of outgoing neutrons:  $\theta_1 = 44.0^\circ, \theta_2 = 44.0^\circ, \phi_{12} = 180^\circ$  (left) and  $\theta_1 = 20.0^\circ, \theta_2 = 116.2^\circ, \phi_{12} = 0^\circ$  (right) as a function of the  $S$ -curve arc length. The SCS NN+3NF  $N^2$ LO predictions are represented by the dashed-dotted curve. The SMS  $N^2$ LO with 3NF of Ref. [24] are given by the dotted curve, while those with 3NF of Ref. [21] are in the centre of the green bands. These bands show the DoB intervals from the  $\tilde{C}_{0.5-10}^{650}$  Bayesian model [21] at DoB level 68%(95%) at NLO: dark yellow band (light yellow band) and at  $N^2$ LO dark green band (light green band). Proton-deuteron data are from Refs. [25] (left) and [26] (right)

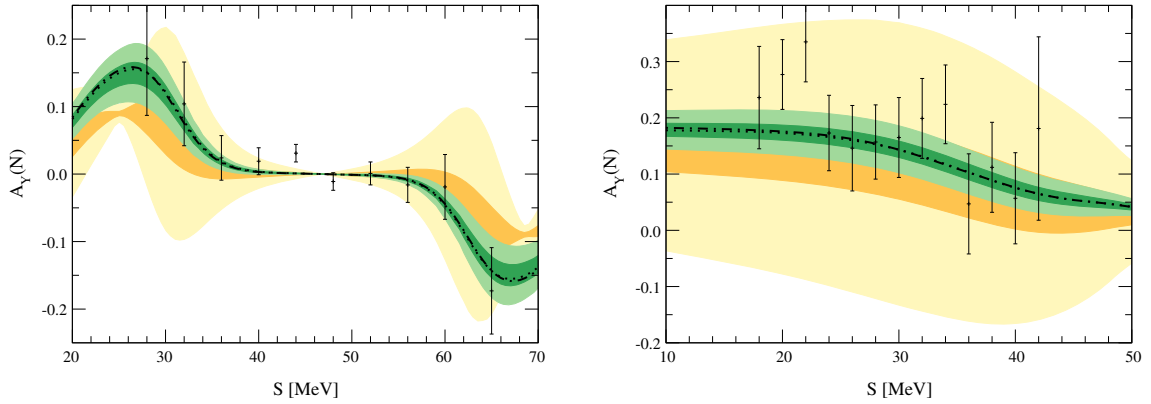


**Fig. 2** The same as in Fig. 1 but for the neutron analyzing power  $A_Y(N)$

are inside the dark band in nearly whole range of the  $S$  parameter. This band determines the truncation error of the SMS predictions and its size results from the Bayesian analysis within the  $\tilde{C}_{0.5-10}^{650}$  model [21] at 68% Degree-of-Belief (DoB) level. Relatively narrow width of that band confirms that in this case no significant contributions from chiral potentials beyond  $N^2$ LO are expected. The data description delivered by chiral forces is satisfactory for one of presented sets of data, but in the case of the  $(\theta_1 = 20.0^\circ, \theta_2 = 116.2^\circ, \phi_{12} = 0^\circ)$  configuration data are outside theoretical uncertainties. In Fig. 2 we give, for the same configurations as in Fig. 1, the neutron vector analyzing power  $A_Y(N)$  as an example of the polarization observable. The picture is similar to the one for the cross section—there is a nice agreement between all the three predictions. The differences between predictions and the sizes of the truncation errors are much smaller than the experimental uncertainties, and data are well described by our results.

With the increasing energy the bigger sensitivity to details of interaction is expected. In Figs. 3 and 4 we show the differential cross section and the deuteron tensor analyzing power  $A_{XZ}$  at the energy  $E=135$  MeV, using the same chiral forces as for Figs. 1 and 2. Also at this energy all tested chiral approaches give similar predictions, well inside the 68% DoB interval. All bands representing truncation errors are now visibly wider than these at  $E=65$  MeV, thus we conclude that at this energy (and above) higher-order chiral forces should be employed.

Indeed, if the  $N^4$ LO<sup>+</sup> two-body force is used instead of the  $N^2$ LO one, a clear shift of predictions is observed. This is illustrated in Figs. 5 and 6, where for the same energy and kinematical configurations as presented in Figs. 3 and 4, we show complete  $N^2$ LO SMS predictions, given by the black dotted curve, and

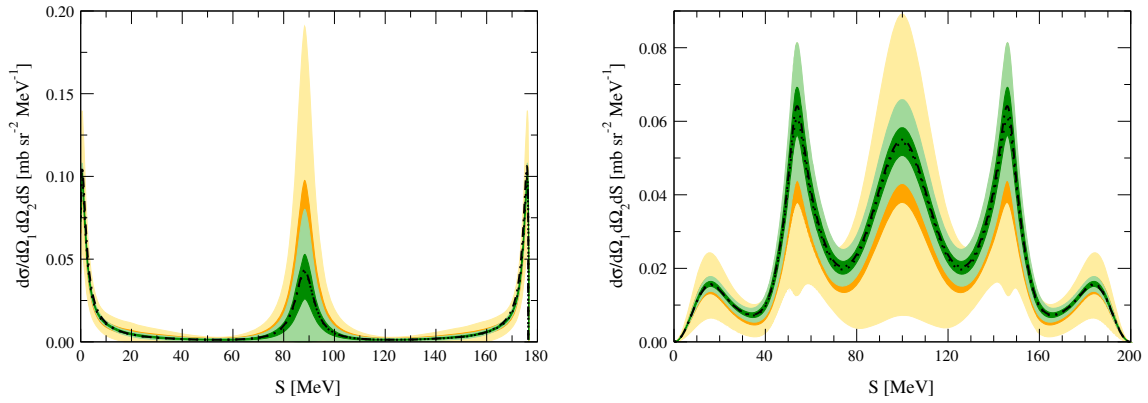


**Fig. 3** The same as in Fig. 1 but for the neutron energy  $E = 135$  MeV and directions of momenta of outgoing neutrons:  $\theta_1 = 15.0^\circ$ ,  $\theta_2 = 15.0^\circ$ ,  $\phi_{12} = 0^\circ$  (left) and  $\theta_1 = 54.4^\circ$ ,  $\theta_2 = 54.4^\circ$ ,  $\phi_{12} = 180^\circ$  (right)

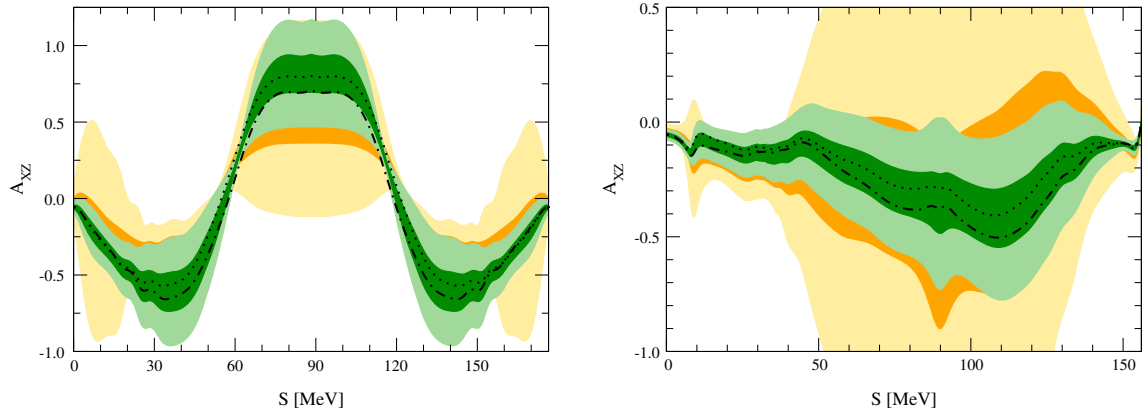


**Fig. 4** The same as in Fig. 3 but for the deuteron tensor analyzing power  $A_{XZ}$  and directions of momenta of outgoing neutrons:  $\theta_1 = 15.0^\circ$ ,  $\theta_2 = 15.0^\circ$ ,  $\phi_{12} = 0^\circ$  (left) and  $\theta_1 = 25.0^\circ$ ,  $\theta_2 = 100.0^\circ$ ,  $\phi_{12} = 180^\circ$  (right)

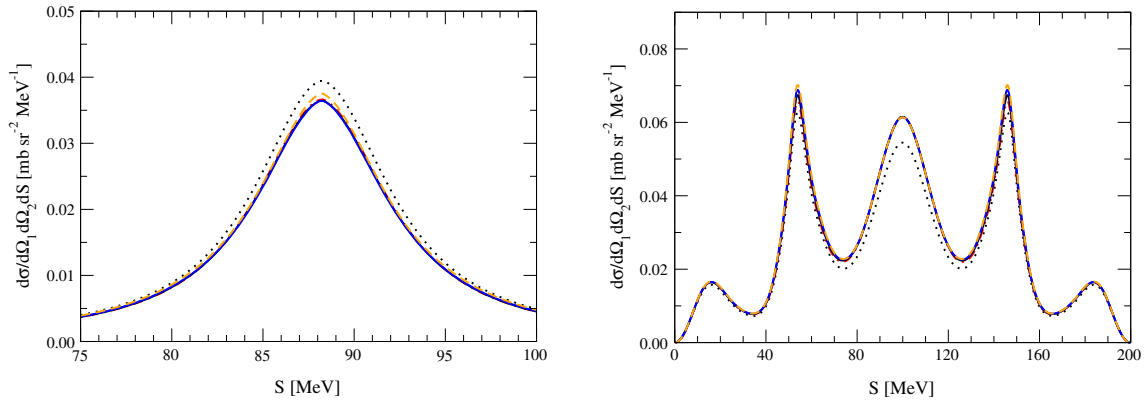


**Fig. 5** The same as in Fig. 3 but red dash-dotted, black solid, blue solid and orange dashed curves represents now NN+3NF predictions with 3NF at  $N^2LO$  combined with NN potential at  $N^4LO^+$  for regulator value  $\Lambda = 400, 450, 500,$  and  $550$  MeV, respectively. The black dotted curve shows complete  $N^2LO$  results at  $\Lambda = 450$  MeV

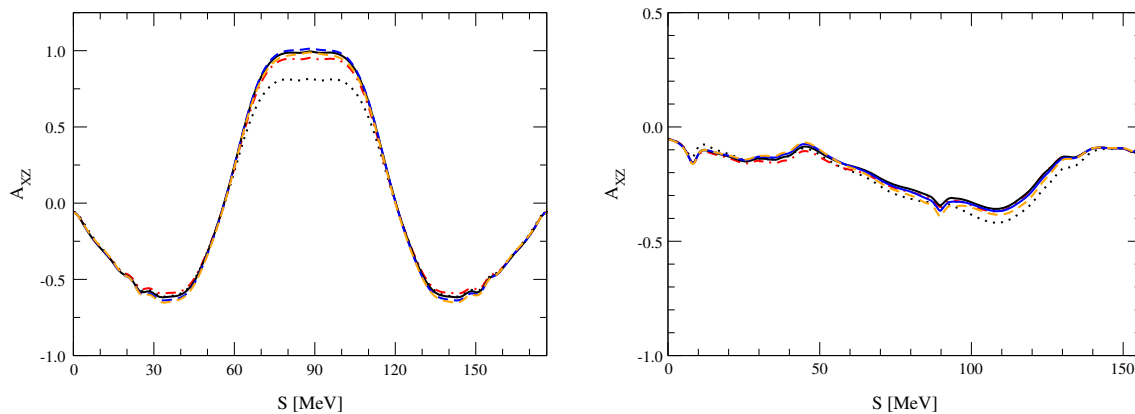


**Fig. 6** The same as in Fig. 4 but with curves as in Fig. 5

incomplete  $N^4LO^+$  results given by the black solid curve, both at  $\Lambda = 450$  MeV. Incompleteness arise from the fact, that we combined here  $N^4LO^+$  NN interaction with the  $N^2LO$  3NF, of course matching free parameters of the 3NF accordingly. The same figures show also a dependence of incomplete calculations on the value of the regulator parameter  $\Lambda$ . Both for the cross section and  $A_{XZ}$  the change of cutoff parameters, and resulting change of 3NF's parameters, affects predictions only slightly. Thus the truncation error remains a dominant source of theoretical uncertainty.

Summarizing, the recent progress in development of chiral NN and 3N forces provided us with the SMS potential which we applied to the neutron induced deuteron breakup. We find the weak dependence on the value of the regulator parameter of the predicted observables and plan to extend the presented studies to complete  $N^3LO$  results. The work in this direction is in progress.

**Acknowledgements** This work is a part of the LENPIC project and was supported by the Polish National Science Center under Grants No. 2016/22/M/ST2/00173. We would like to thank Dr. A. Nogga for providing us the matrix elements of the SMS 3NF. The numerical calculations were partially performed on the supercomputer cluster of the JSC, Jülich, Germany.

**Open Access** This article is licensed under a Creative Commons Attribution 4.0 International License, which permits use, sharing, adaptation, distribution and reproduction in any medium or format, as long as you give appropriate credit to the original author(s) and the source, provide a link to the Creative Commons licence, and indicate if changes were made. The images or other third party material in this article are included in the article's Creative Commons licence, unless indicated otherwise in a credit line to the material. If material is not included in the article's Creative Commons licence and your intended use is not permitted by statutory regulation or exceeds the permitted use, you will need to obtain permission directly from the copyright holder. To view a copy of this licence, visit <http://creativecommons.org/licenses/by/4.0/>.

## References

1. S. Weinberg, Effective chiral Lagrangians for nucleon - pion interactions and nuclear forces. *Nucl. Phys. B* **363**, 3–18 (1991)
2. E. Epelbaum, U.G. Meißner, Chiral dynamics of few- and many-nucleon systems. *Ann. Rev. Nucl. Part. Sci.* **62**, 159–185 (2012)
3. E. Epelbaum, H. Krebs, P. Reinert, High-precision nuclear forces from chiral EFT: state-of-the-art, challenges and outlook. *Front. Phys.* **8**, 98 (2020)
4. E. Epelbaum, W. Glöckle, U.G. Meißner, Nuclear forces from chiral Lagrangians using the method of unitary transformation (I): formalism. *Nucl. Phys. A* **637**, 107–134 (1998)
5. E. Epelbaum, W. Glöckle, U.G. Meißner, The two-nucleon system: Nuclear forces from chiral Lagrangians using the method of unitary transformation II. *Nucl. Phys. A* **671**, 295–331 (2000)
6. E. Epelbaum, W. Glöckle, U.G. Meißner, The two-nucleon system at next-to-next-to-next-to-leading order. *Nucl. Phys. A* **747**, 362–424 (2005)
7. E. Epelbaum et al., Three nucleon forces from chiral effective field theory. *Phys. Rev. C* **66**, 064001-1–17 (2002)
8. R. Skibiński et al., The chiral long-range two-pion exchange electromagnetic currents in radiative nucleon-deuteron capture. *Acta Phys. Pol. B* **46**, 159–168 (2015)
9. D. Rozpędzik et al., Signatures of the chiral two-pion exchange electromagnetic currents in the 2H and 3He photodisintegration reactions. *Phys. Rev. C* **83**, 064004-1–10 (2011)
10. R. Skibiński et al., The triton with long-range chiral  $N^3LO$  three nucleon forces. *Phys. Rev. C* **84**, 054005-1–10 (2011)
11. H. Witała et al., Calculations of three-nucleon reactions with  $N^3LO$  chiral forces: achievements and challenges. *J. Phys. G Nucl. Part. Phys.* **41**, 094011-1–21 (2014)

12. J. Golak et al., Low-energy neutron-deuteron reactions with  $N^3$ LO chiral forces. *Eur. Phys. J. A* **50**, 177–1–11 (2014)
13. E. Epelbaum, H. Krebs, U.-G. Meißner, Improved chiral nucleon-nucleon potential up to next-to-next-to-next-to-leading order. *Eur. Phys. J. A* **51**, 53–81 (2015)
14. E. Epelbaum, H. Krebs, U.-G. Meißner, Precision nucleon-nucleon potential at fifth order in the chiral expansion. *Phys. Rev. Lett.* **115**, 122301-1–5 (2015)
15. E. Epelbaum et al., Few- and many-nucleon systems with semilocal coordinate-space regularized chiral two- and three-body forces. *Phys. Rev. C* **99**, 024313-1–13 (2019)
16. P. Reinert et al., Semilocal momentum-space regularized chiral two-nucleon potentials up to fifth order. *Eur. Phys. J. A* **54**, 86–49 (2018)
17. M. Hoferichter et al., Matching Pion-Nucleon Roy-Steiner Equations to Chiral Perturbation Theory. *Phys. Rev. Lett.* **115**, 192301-1–6 (2015)
18. R. Navarro Pérez, J.E. Amaro, E. Ruiz Arriola, Statistical error analysis for phenomenological nucleon-nucleon potentials. *Phys. Rev. C* **89**, 064006-1–20 (2014)
19. Yu. Volkotrub et al., Uncertainty of three-nucleon continuum observables arising from uncertainties of two-nucleon potential parameters. *J. Phys. G Nucl. Part. Phys.* **47**, 104001-1–19 (2020)
20. Y. Volkotrub *et al.*, these proceedings
21. P. Maris et al., Light nuclei with semilocal momentum-space regularized chiral interactions up to third order. *Phys. Rev. C* **103**, 054001-1–20 (2021)
22. W. Glöckle et al., The three-nucleon continuum: achievements, challenges and applications. *Phys. Rep.* **274**, 107–285 (1996)
23. W. Glöckle, *The Quantum Mechanical Few-Body Problem* (Springer, Berlin, 1983)
24. E. Epelbaum et al., Towards high-order calculations of three-nucleon scattering in chiral effective field theory. *Eur. Phys. J. A* **56**, 92 (2020)
25. M. Allet et al., Proton-induced deuteron breakup at  $E_p^{lab} = 65$  MeV in Quasi-free scattering configurations. *Few Body Syst.* **20**, 27–40 (1996)
26. K. Bodek et al., Proton-induced deuteron breakup reaction at 65 MeV: unspecific configurations. *Few Body Syst.* **30**, 65–79 (2001)